Spatially Variant Morphological Image Processing: Theory and Applications

N. Bouaynaya and D. Schonfeld

Department of Electrical and Computer Engineering, University of Illinois at Chicago, Chicago, USA.

ABSTRACT

Originally, mathematical morphology was a theory of signal transformations which are invariant under Euclidean translations. An interest in the extension of mathematical morphology to spatially-variant (SV) operators has emerged due to the requirements imposed by numerous applications in adaptive signal (image) processing. This paper presents a general theory of spatially-variant mathematical morphology in the Euclidean space. We define the binary and gray-level spatially-variant basic morphological operators (i.e., erosion, dilation, opening and closing) and study their properties. We subsequently derive kernel representations for a large class of binary and gray-level SV operators in terms of the basic SV morphological operators. The theory of SV mathematical morphology is used to extend and analyze two important image processing applications: morphological image restoration and skeleton representation of binary images. For morphological image restoration, we obtain new realizations of adaptive median filters in terms of the basic SV morphological operators. For skeleton representation, we develop an algorithm to construct the optimal structuring elements, in the sense of minimizing the cardinality of the spatially-variant morphological skeleton representation. Experimental results show the power of the proposed theory of spatially-variant mathematical morphology in practical image processing applications.

Keywords: Spatially-Variant Mathematical Morphology, Spatially-variant homomorphism theorem, Kernel representation, Adaptive median filter, Spatially-Variant skeleton representation.

1. INTRODUCTION

Since first introduced by Matheron and Serra[1 2 3] in the 70's, mathematical morphology theory has found numerous applications in signal and image processing, which include biomedical image processing,[4] shape recognition and analysis,[5] coding and compression,[6] automated industrial inspection,[7] texture analysis,[8] radar imagery,[9] astronomical imaging,[10] multiresolution techniques and scale-spaces.[11] Despite the diversity of purposes, the above applications have a common goal: extract shape information from images.

Mathematical morphology in its original form is a set-theoretic approach to image analysis which investigates the geometrical structure of images. Morphological image transformations have an intuitive geometrical interpretation and can be represented by two elementary operators[2 12] [*]: *erosions* and *dilations*. This enables the implementation of efficient and low-complexity algorithms of the transformations.[13] To examine the geometrical structure of an image, a small pattern, called *structuring element*, is translated over the image to extract useful information. Therefore, morphological operators are invariant under translations.

Translation-invariant transformations are not appropriate for many applications in image processing. For instance, in the analysis of images from traffic control cameras, vehicles at the bottom of the image are closer to the camera and thus appear larger than vehicles higher in the image.[14] Therefore, the structuring element should vary linearly with the vertical position in the image in order to detect and extract vehicles from the image. Another example arises in adaptive smoothing of noisy signals, which consists of removing the noise while preserving the image features. This can be achieved by varying the filtering scales (i.e., the structuring elements) with respect to spatial positions in the image[15 16] .[17]

Several methods for the extension of mathematical morphology have consequently been proposed to spatially-variant operators restricted by various rigid algebraic constructions such as circular morphology[18] and affine morphology.[19] Roedrink constructed and studied morphological operators which are invariant under more

[*] We will use operator, transformation, and system interchangeably to denote a signal-to-signal transformation.

general non-commutative groups, such as the projective group and the motion group.[20] A unified theory of spatially-variant mathematical morphology requires nonetheless a further abstraction of the basic notions of mathematical morphology. Lattice morphology, introduced by Serra[1] and pursued by Heijmans and Ronse,[18 21] is a powerful tool to the analysis of an abstraction of mathematical morphology based on lattice theory, a topic devoted to the investigation of the algebraic properties of partially-ordered sets.[22] A fundamental result in lattice morphology that provides for the representation of a large class of nonlinear operators in terms of lattice erosions and dilations has been presented in.[23] This representation however does not posses the geometrical interpretation captured by the structuring element that is crucial in signal and image processing applications. Motivated by practical applications, Serra[1] introduced the concept of a structuring function in the Euclidean space, which associates to each point in space a local structuring element. This work was pursued by Chefchaouni and Schonfeld in[24] .[25] The latter approach, despite its restriction to the Euclidean space, preserves the geometrical concept of the structuring element that is essential in practical implementation of morphological operators in software and hardware.

In this paper, we provide a formal framework for the theory of spatially-variant mathematical morphology in the Euclidean space. Particularly, we construct the binary (two-level) and gray-level (multi-level) basic spatially-variant morphological operators (i.e., erosion and dilation) and study their properties. We subsequently derive a kernel representation for a large class of binary and gray-level spatially-variant (non necessarily translation-invariant) signal transformations. The proposed theory of spatially-variant mathematical morphology is used to extend and analyze two important image processing applications: morphological image restoration and morphological skeleton representation.

2. PRELIMINARIES

A binary (two-level valued) signal or image can be represented as a set. For example, consider a digital binary image I taking values 0 or 1. The set $A = \{x \in \mathbb{Z}^2 : I(x) = 1\}$ uniquely characterizes the image I. A gray-level (multi-level valued) signal can be represented by a function. The support of such a function is defined as $\mathrm{Spt}(f) = \{x : f(x) \neq -\infty\}$. A binary operator is a transformation that maps a set to a set. A gray-level operator is a transformation that maps a function to a function.

In the binary case, we consider a non-empty set ξ. the power set of ξ is $\mathcal{P}(\xi)$. We use $\mathcal{O} = \mathcal{P}(\xi)^{\mathcal{P}(\xi)}$ to denote the set of all operators mapping $\mathcal{P}(\xi)$ into itself. Elements of the set $\mathcal{P}(\xi)$ will be denoted by upper-case letters; e.g., A, B, C. An order on $\mathcal{P}(\xi)$ is imposed by the inclusion $\subseteq$. We use $\cup$ and $\cap$ to denote the union and intersection in $\mathcal{P}(\xi)$, respectively. X^c denotes the complement of $X \in \mathcal{P}(\xi)$. Elements of the set $\mathcal{O}$ will be denoted by lower case Greek letters; e.g., α, β, γ. We shall restrict our attention to non-degenerate operators; i.e., $\alpha(X) \neq \xi$ and $\alpha(X) \neq \emptyset$ for some $X \in \mathcal{P}(\xi)$ and $\alpha(\emptyset) = \emptyset$, for every $\alpha \in \mathcal{O}$ (the set $\emptyset \in \mathcal{P}(\xi)$ is used to denote the empty set). The operator $\psi^* \in \mathcal{O}$ is the dual of the operator $\psi \in \mathcal{O}$ if and only if (iff) $\psi^*(X) = (\psi(X^c))^c$, for every $X \in \mathcal{P}(\xi)$. An operator $\psi \in \mathcal{O}$ is increasing iff $X \subseteq Y \Longrightarrow \psi(X) \subseteq \psi(Y)$, for every $X, Y \in \mathcal{P}(\xi)$.

In the gray-level case, we consider functions from $\xi = \mathbb{R}^n$ or $\xi = \mathbb{Z}^n$, for some $n > 0$, to $\mathcal{T} = \mathbb{Z}$ or $\mathcal{T} = \mathbb{R}$. We denote the set of functions from ξ to $\mathcal{T}$ by *Func* $(\xi, \mathcal{T})$. Elements of *Func* $(\xi, \mathcal{T})$ will be denoted by lower-case letters; e.g., f, g. An order on *Func* $(\xi, \mathcal{T})$ is induced by the order on $\mathcal{T}$; that is $f \leq g \Longleftrightarrow f(x) \leq g(x)$, for every $x \in \xi$. The least and greatest elements of *Func* $(\xi$,T) are denoted by $\mathcal{O}$ and $\mathcal{I}$; these are the functions identically $-\infty$ and $+\infty$, respectively. $\vee$ and $\wedge$ denote the supremum and infimum operations, respectively. If $\{f_i\}_{i \in I}$ is a family of functions in *Func* $(\xi, \mathcal{T})$, then $(\vee_{i \in I} f_i)(x) = \vee_{i \in I}\{f_i(x)\}$ and $(\wedge_{i \in I} f_i)(x) = \wedge_{i \in I}\{f_i(x)\}$. Gray-level operators will be denoted by upper-case Greek letters; e.g., Ψ, Φ. We consider only non-degenerate operators; i.e., $\Psi(f) \neq \mathcal{O}$, $\Psi(f) \neq \mathcal{I}$, for some function f, $\Psi(\mathcal{O}) = \mathcal{O}$ and $\Psi(\mathcal{I}) = \mathcal{I}$ for every gray-level operator Ψ. The dual operator Ψ^* of a gray-level operator Ψ is defined as $\Psi^*(f) = -\Psi(-f)$, for all $f \in$ *Func* $(\xi, \mathcal{T})$.

3. SPATIALLY-VARIANT MORPHOLOGY

3.1. Spatially-Variant Binary Morphological Operators

The spatially-variant binary structuring element θ is a mapping from ξ to $\mathcal{P}(\xi)$, which associates to each point in space x a local structuring element $\theta(x)$. We define the transposed mapping θ' as

$$\theta'(y) = \{z \in \xi : y \in \theta(z)\}, \quad \text{for every } y \in \xi. \tag{1}$$

In the translation invariant case, the mapping θ is the translation by a fixed set B, i.e., $\theta(x) = B_x$, for every $x \in \xi$. Then, we have $y \in \theta^{'}(x) \Longleftrightarrow x \in \theta(y) \Longleftrightarrow x \in B_y \Longleftrightarrow y \in \check{B}_x$. Hence, the transposed mapping is the translation by the reflected set $\check{B}$. The four basic spatially-variant (SV) binary operators are defined as

SV binary erosion: $\mathcal{E}_\theta(X) = \{z \in \xi : \theta(z) \subseteq X\} = \bigcap_{x \in X^c} \theta'^c(x), \quad$ for every $X \in \mathcal{P}(\xi)$,

SV binary dilation: $\mathcal{D}_\theta(X) = \{z \in \xi : \theta^{'}(z) \cap X \neq \emptyset\} = \bigcup_{x \in X} \theta(x), \quad$ for every $X \in \mathcal{P}(\xi)$,

SV binary opening: $\Gamma_\theta(X) = \mathcal{D}_\theta(\mathcal{E}_\theta(X)) = \bigcup\{\theta(y) : \theta(y) \subseteq X; y \in \xi\}$,

SV binary closing: $\Phi_\theta(X) = \mathcal{E}_\theta(\mathcal{D}_\theta(X)) = \{z \in \xi : \theta(y) \cap X \neq \emptyset,$ for every $\theta(y) : z \in \theta(y)\}$.

3.1.1. Properties of spatially-variant binary erosion and dilation

- *Adjunction*: $\mathcal{D}_\theta(X) \subseteq Y \Longleftrightarrow X \subseteq \mathcal{E}_\theta(Y)$,
- *Duality*: $\mathcal{E}^*_\theta = \mathcal{D}_{\theta'}$,
- *Increasing*: If $X \subseteq Y$, then $\mathcal{E}_\theta(X) \subseteq \mathcal{E}_\theta(Y)$ and $\mathcal{D}_\theta(X) \subseteq \mathcal{D}_\theta(Y)$,
- If $\theta_1 \subseteq \theta_2$, then $\mathcal{E}_{\theta_2} \subseteq \mathcal{E}_{\theta_1}$ and $\mathcal{D}_{\theta_1} \subseteq \mathcal{D}_{\theta_2}$.

3.1.2. Properties of spatially-variant binary opening and closing

- *Duality*: $\Gamma^*_\theta = \Phi_{\theta'}$,
- *Increasing*: If $X \subseteq Y$, then $\Gamma_\theta(X) \subseteq \Gamma_\theta(Y)$ and $\Phi_\theta(X) \subseteq \Phi_\theta(Y)$,
- *Idempotence*: $\Gamma_\theta(\Gamma_\theta) = \Gamma_\theta$ and $\Phi_\theta(\Phi_\theta) = \Phi_\theta$,
- *Extensivity and Anti-extensivity*: $\Gamma_\theta(X) \subseteq X$ and $X \subseteq \Phi_\theta(X)$.

Observe that the spatially-variant binary morphological operators satisfy the same properties as their translation-invariant counterparts.

3.2. Spatially-Variant Gray-Level Morphological Operators

Spatially-variant binary morphological operators can be naturally extended to gray-level signals by means of the umbra approach. The umbra of a function f, denoted as $U[f]$ is defined as

$$U[f] = \{(x, y) \in \xi \times \mathbb{Z} : y \leq f(x)\}. \tag{2}$$

More generally, we call a set $V \subseteq \xi \times calT$ an umbra if $(x, y) \in V \longleftrightarrow (x, t) \in V, \ \forall\, t \leq y$. Obviously, the umbra of a function is an umbra. To any umbra V, we define its top surface, a function $T[V] : \xi \to \mathcal{T}$, whose graph is the upper envelope of V, i.e.

$$T[V](x) = \vee\{y \in \mathbb{Z} : (x, y) \in U[f]\}. \tag{3}$$

Clearly $T[U[f]] = f$ for any function f. However, we do not have in general $V = U[T[V]]$ for any umbra V. The relation between umbras and functions is different in the two cases of discrete and continuous gray-levels.[26] If the gray-level space $\mathcal{T} = \mathbb{Z}$, then we have $V = U[T[V]]$ for any umbra V. Thus, there is a bijection between functions and umbras where a function f and an umbra V correspond by the equivalent relation $V = U[f] \leftrightarrow f = T[V]$. If the gray-level space $\mathcal{T} = \mathbb{R}$, then the bijection between functions and umbras holds only for upper-semi-continuous functions. A function $f : \xi \to R$ is said to be upper-semi-continuous (u.s.c.) if for every $h \in \xi$, we have $\limsup_{x \to h} f(x) \leq f(h)$ or equivalently if its umbra is closed in $\xi \times \mathbb{R}$. Observe that discrete domain functions are trivially upper-semi-continuous. In the reminder of this paper, we will consider only upper-semi-continuous functions. We denote by $USC(\xi, \mathcal{T})$ the set of upper-semi-continuous functions from ξ to $\mathcal{T}$.

The spatially-variant structuring function Θ [†] is a mapping from ξ to $USC\ (\xi, \mathcal{T})$, which associates to each point x a local structuring function $\Theta(x)$. We define the transposed structuring function mapping Θ' as $[\Theta^{'}(x)](u) = [\Theta(u)](x)$ for all $x, u \in \xi$. In translation-invariant gray-level morphology, the mapping Θ is the translation by a fixed structuring function g, i.e., $[\Theta(x)](u) = g(u - x) = g(u)_x$, for every $x \in \xi$. Then $[\Theta^{'}(u)](x) = [\Theta(x)](u) = g(u - x)$, for every $x \in \xi$; that is $[\Theta^{'}(u)] = \breve{g}_u$, for every $u \in \xi$. Hence the transposed mapping $\Theta^{'}$ is the translation by the structuring function $\breve{g}$, where $\breve{g}(x) = g(-x)$, for every $x \in \xi$. We define the umbra structuring element Θ^U as the following mapping

$$\Theta^U(x, y) = U[\Theta(x) + y] = U[\Theta(x)] + y. \tag{4}$$

Consequently, the structuring elements in the space $\xi \times \mathcal{T}$ are invariant along the vertical (gray-level) axis.
Proposition 1. For every umbra V, $\mathcal{E}_{\Theta^U}(V)$ and $\mathcal{D}_{\Theta^U}(V)$ are umbras.
Definition 1. The spatially-variant gray-level erosion is defined, for every $f \in USC(\xi, \mathcal{T})$, for every $x \in \xi$, as

$$[\mathcal{E}_\Theta(f)](x) = T[\mathcal{E}_{\Theta^U}(U[f])](x) = \bigwedge_{u \in \mathrm{Spt}(\Theta(x))} \{f(u) - [\Theta(x)](u)\} = \vee\{v \in \mathcal{T} : \Theta(x) + v \leq f\}. \tag{5}$$

Definition 2. The spatially-variant gray-level dilation is defined, for every $f \in USC(\xi, \mathcal{T})$, for every $x \in \xi$, as

$$[\mathcal{D}_\Theta(f)](x) = T[\mathcal{D}_{\Theta^U}(U[f])](x) = \bigvee_{u \in \mathrm{Spt}(f) \cap \mathrm{Spt}(\Theta^{'}(x))} \{f(u) + [\Theta^{'}(x)](u)\} = \wedge\{v \in \mathcal{T} : -\Theta'(x) + v \geq f\}. \tag{6}$$

Observe that, except for $\mathcal{T} = \mathbb{Z}$, Definitions 1 and 2 do not necessarily imply that $U[\mathcal{E}_\Theta(f)] = \mathcal{E}_{\Theta^U}(U[f])$ and $U[\mathcal{D}_\Theta(f)] = \mathcal{D}_{\Theta^U}(U[f])$. A sufficient condition to ensure these relations is that $\mathcal{E}_\Theta(f)$ and $\mathcal{D}_\Theta(f)$ are upper-semi-continuous functions or equivalently that $\mathcal{E}_{\Theta^U}(U[f])$ and $\mathcal{D}_{\Theta^U}(U[f])$ are closed umbras for every upper-semi-continuous function f. Before stating the spatially-variant umbra homomorphism theorem, we need the following definition. We say that the mapping Θ is sequentially continuous if for every sequence $\{x_n\}_{n \in \mathbb{N}} \in \xi$ converging towards the point $x \in \xi$, the sequence of upper-semi-continuous functions $\{\Theta(x_n)\}_{n \in \mathbb{N}}$ converges towards the upper-semi-continuous function $\Theta(x)$ in the sense specified by Serra [p.429, Theorem XII-2].[3]
Spatially-Variant Umbra Homomorphism theorem 3. Let $\Theta : \xi \to USC(\xi, \mathcal{T})$ be a sequentially continuous structuring function mapping. Then, for every $f \in USC(\xi, \mathcal{T})$,
(a) $U[\mathcal{E}_\Theta(f)] = \mathcal{E}_{\Theta^U}(U[f])$.
(b) If the support of $\Theta'(x)$ is compact for every $x \in \xi$, then $U[\mathcal{D}_\Theta(f)] = \mathcal{D}_{\Theta^U}(U[f])$.

The spatially-variant umbra homomorphism theorem states that, under the specified conditions, the operation of taking an umbra is a homomorphism from the SV gray-level morphology to the SV binary morphology.
Proposition 2. The spatially-variant gray-level pair $(\mathcal{E}_\Theta, \mathcal{D}_\Theta)$ forms an adjunction, i.e.,

$$\mathcal{D}_\Theta(f) \leq g \iff f \leq \mathcal{E}_\Theta(g), \quad \text{for every } f, g \in USC(\xi). \tag{7}$$

Proposition 1 implies in particular that $\mathcal{E}_\Theta$ is an erosion (commutes with the infimum) and that $\mathcal{D}_\Theta$ is a dilation (commutes with the supremum).
Proposition 3. The spatially-variant gray-level erosion and dilation are dual operators, i.e., $\mathcal{E}^*_\Theta = \mathcal{D}_{\Theta'}$.

Proposition 4. The spatially-variant gray-level erosion and dilation are increasing operators.
From Definitions 1 and 2, we can construct the SV opening and closing as follows
Definition 3. The spatially-variant gray-level opening is defined, for every $f \in USC(\xi, \mathcal{T})$, as

$$\Gamma_\Theta(f) = \mathcal{D}_\Theta(\mathcal{E}_\Theta(f)) = \Gamma_\Theta(f) = \vee\{\Theta(u) + v \leq f; (u, v) \in \xi \times \mathcal{T}\}. \tag{8}$$

Definition 4. The spatially-variant gray-level closing is defined, for every $f \in USC(\xi, \mathcal{T})$, as

$$\Phi_\Theta(f) = \mathcal{E}_\Theta(\mathcal{D}_\Theta(f))(x) = \wedge\{\Theta'(u) + v \geq f; (u, v) \in \xi \times \mathcal{T}\}. \tag{9}$$

Hence, the SV gray-level opening and closing have an intuitive geometric interpretation in the same manner

[†]Notice that we are using lower case letter θ to denote the spatially-variant structuring element mapping and upper case letter Θ to denote the spatially-variant structuring function mapping.

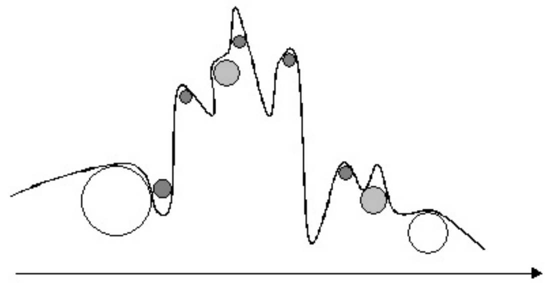

Figure 1. 1-D Geometric Interpretation of SV gray-level opening using circular structuring element mapping

that there is a geometric meaning to the their translation-invariant counterparts. The SV gray-level opening of a function f by the structuring function mapping Θ is obtained by sliding the local structuring functions $\Theta(x)$ under the surface of f and taking the locus of the highest points reached by any part of $\Theta(x)$ as it slides. For instance, Fig. 1 shows a 1-D example of SV gray-level opening using a circular structuring element mapping. The SVFP closing has the dual interpretation, i.e., it is the locus of the lowest points reached by some parts of the transposed local structuring functions $\Theta'(x)$ during the sliding on top of the surface of f. From Propositions 3 and 4, it follows that the SV opening and closing are increasing dual operators.

Proposition 5. The spatially-variant gray-level opening (resp. closing) is anti-extensive (resp. extensive), i.e.,

$$\Gamma_\Theta(f) \leq f, \text{ and } \Phi_\Theta(f) \geq f, \text{ for every } f \in \mathit{USC}(\xi, \mathcal{T}). \tag{10}$$

Proposition 6. The spatially-variant gray-level opening and closing are idempotent operators, i.e., for every $f \in \mathit{USC}(\xi, \mathcal{T})$,

$$\Gamma_\Theta(\Gamma_\Theta(f)) = \Gamma_\Theta(f), \text{ and } \Phi_\Theta(\Phi_\Theta(f)) = \Phi_\Theta(f). \tag{11}$$

4. SPATIALLY-VARIANT KERNEL REPRESENTATION

We extend the notion of the kernel to spatially-variant operators. Let $\psi \in \mathcal{O}$ be a spatially-variant operator, then $Ker\ (\psi) = \{\theta : z \in \psi(\theta(z)), \text{ for every } z \in \xi\}$. We extend Matheron's kernel representation theorem as follows

Theorem 4. Let ψ be an increasing spatially-variant binary operator ψ, which satisfies $\psi(\xi) = \xi$. Then, for every $X \in \mathcal{P}(\xi)$,

$$\psi(X) = \bigcup_{\theta \in Ker\ (\psi)} \mathcal{E}_\theta(X) = \bigcap_{\theta \in Ker\ (\psi^*)} \mathcal{D}_{\theta'}(X). \tag{12}$$

Definition 5. A gray-level operator Ψ is a V-operator if and only if we have $\Psi(f+y) = \Psi(f)+y$, for every $f \in$ *Func* $(\xi, \mathcal{T})$ and every $y \in \mathcal{T}$.

For example, the spatially-variant gray-level erosion, dilation, opening and closing are V-operators. V-operators have been extensively used in many adaptive filtering applications[17] [15] .[16] They are invariant with respect to DC biases and they have an intuitive geometric interpretation.

Let Ψ be a V-operator. We define the kernel $\mathcal{K}(\Psi)$ of Ψ to be the following collection of mappings: $\mathcal{K}(\Psi) = \{\Theta : \Psi[\Theta(x)](x) \geq 0, \text{ for all } x \in \xi\}$. We extend Maragos' kernel representation theorem as follows

Theorem 5. Let Ψ be an increasing V-operator. Then, for every for every $f \in \mathit{USC}(\xi, \mathcal{T})$,

$$\Psi(f) = \bigvee_{\theta \in \mathcal{K}(\Psi)} \mathcal{E}_\Theta(f) = \bigwedge_{\Theta \in \mathcal{K}(\Psi^*)} \mathcal{D}_{\Theta'}(f). \tag{13}$$

Theorems 3 and 4 demonstrate the ubiquity of the SV binary and gray-level morphological operators. Hence the theory of SV mathematical morphology is very general and applies to all binary (resp. gray-level) operators that share two properties: increasing, i.e., preserve a signal ordering, and fixing the entire space (resp. invariant under gray-level translations). Moreover, such decompositions of non-linear operators in terms of elementary ones allows fast and efficient implementations on digital computers, which explains the practical importance of Theorems 3 and 4. For example, the industrial need in automated visual systems requires low-cost machine vision modules, which can perform different complex image processing/analysis tasks based on a small set of available simple operations. Given the parallelism and simple implementation of the SV erosion and dilation, the representation theorems support a general purpose vision (software and hardware) module.

5. APPLICATIONS

5.1. Adaptive Median Filter

5.1.1. Theoretical Analysis

Consider $\xi \subseteq \mathbb{Z}^2$. Let B be a mapping from ξ into $\mathcal{P}(\xi)$ such that $y \in B(y)$ and $|B(y)| =$ cardinality $B(y) = n$, for every $y \in \xi$ where n is odd. The spatially-variant or adaptive binary median filter is given by

$$med(X, B) = \{y \in \xi : |X \cap B(y)| \geq (n+1)/2\}. \quad (14)$$

The corresponding adaptive gray-level median filter is given by

$$[med(f, B)](x) = (n+1)/2 \text{ largest value of} \{f(y), y \in B(x)\}. \quad (15)$$

Proposition 7. The spatially-variant binary and gray-level median filters are increasing self-dual operators .

Moreover, we observe that $med(\xi, B) = \xi$ and $med(f, B)$ is a V-operator. Therefore, Theorems 4 and 5 apply, respectively, to the adaptive binary median filter and to the adaptive gray-level median filter.
Proposition 8.

$$med(X, B) = \bigcup_{\theta \subseteq B, |\theta| = (|B|+1)/2} \; \bigcap_{x \in X^c} \theta'^c(x) = \bigcap_{\theta \subseteq B, |\theta| = (|B|+1)/2)} \; \bigcup_{x \in X} \theta(x), \quad (16)$$

for every $X \in \mathcal{P}(\xi)$, and

$$[med(f, B)](x) \;\; = \bigvee_{\theta \subseteq B, |\theta| = (|B|+1)/2} [\bigwedge_{u \in \theta(x)} f(u)] = \bigwedge_{\theta \subseteq B, |\theta| = (|B|+1)/2} [\bigvee_{u \in \theta(x)} f(u)], \quad (17)$$

for every $f \in Func(\xi, \mathcal{T})$.
The implications of Eqs. (16) and (17) are profound because they enable us to express any adaptive median filter in a closed formula involving only max-min (or union-intersection) operations. In particular, no sorting is required. For small adaptive window sizes B, the kernel representation is more efficient than sorting schemes.[12]

5.1.2. Simulations

We assume a germ-grain degradation process $\Theta(\bullet)^2$.[27] The output Y of $\Theta(\bullet)$ is given by

$$Y = \Theta(X) = (X - N_1) \cup N_2, \quad \text{where} \quad N_i = \bigcup_{n=1,2,\cdots} C_{i,n} + \{x_{i,n}\}, \quad i = 1, 2. \quad (18)$$

In this case $\{C_{i,n}, n = 1, 2, \cdots\}$ is a sequence of sets, known as the primary grains, whereas $\{x_{i,n}, n = 1, 2, \cdots\}$ is a sequence of sites, known as the germs, which are randomly distributed in $\mathbb{Z}^2$.

The idea of our implementation of the adaptive median filter is to select a local window with size slightly larger than the noise structures. The degraded pixels are replaced by the median value computed in the local window while the intact pixels are left unfiltered. Recall that a good adaptive filtering scheme should be able to eliminate noise without oversmoothing the important features of signals. For each pixel x, detect if a noise-grain $C(x)$ is centered at x. If yes: Let $B(x) = C(x) \oplus S$. Otherwise: $B(x) = \emptyset$. The detection of the presence of a noise-grain $C(x)$ centered at the pixel x is determined by selecting the largest possible grain C in the germ-grain model given by (18) which is present or absent in the degraded image (i.e., $C + \{x\} \subseteq Y$ or $C + \{x\} \subseteq Y^c$).[28]

We consider the original image depicted in Fig. 2(a). Its corrupted version by a germ-grain noise model is shown in Fig. 2(b). The germ-grains are randomly distributed squares of size 1, 3, 5 and 7. The noise grains are allowed to overlap. Figures 2(c) - 2(e) show the output of translation-invariant median filtering with square windows of sizes 5×5, 7×7 and 9×9, respectively. Observe that median filters with larger windows remove more noise at the cost of oversmoothing the output image. This is a known trade-off between the noise removal capability of translation-invariant median filters and their degree of smoothness of the original image. The spatially-variant median filtering output is depicted in Figure 2(f). The SV median filter removes all germ-grain noise while preserving the edges and the geometry of the original image. Table 1 displays the signal-to-noise ratio (SNR) of the filtered images.

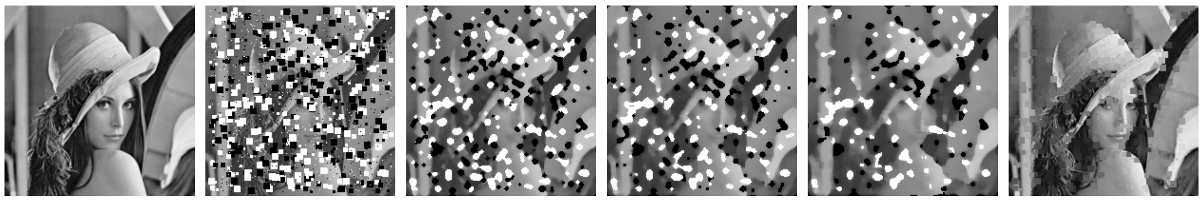

(a) (b) (c) (d) (e) (f)

Figure 2. Median filtering: a) Original image; b) Degraded image by a germ-grain noise model; c) Translation-invariant median filtering using a fixed 5×5 square window; d) Translation-invariant median filtering using a fixed square 7×7 window; e) Translation-invariant median filtering using a fixed 9×9 square window; f) Adaptive median filtering.

Image	SNR (dB)
(b) Degraded Image	9.37
(d) Translation-invariant median filtering using a fixed 5×5 window	11.96
(e) Translation-invariant median filtering using a fixed 7×7 window	13.08
(f) Translation-invariant median filtering using a fixed 9×9 window	15.10
(g) Spatially-Variant median filtering	40

Table 1. Denoising using median filtering: SNR comparison

5.2. Spatially-Variant Morphological Skeleton Representation

The translation-invariant morphological skeleton has been investigated by many researchers[3, 29, 30, 31] mainly for the purpose of image coding and shape recognition. An important subject in morphological skeleton decomposition of binary images is the issue of minimal skeletons. In many applications of interest (e.g., image coding), it is desirable to develop an image decomposition which contains the minimum possible number of points that are sufficient for the exact reconstruction of the original image. In this section, we generalize the morphological skeleton representation to the spatially-variant morphological skeleton representation. We also develop an algorithm for its implementation, which minimizes the cardinality of the image representation.

5.2.1. Theoretical Analysis

Consider a sequence of mappings $\{B_n : n \geq 0\}$ from ξ into $\mathcal{P}(\xi)$ such that $z \in B_n(z)$, for every $z \in \xi$, for all n and $B_n(z) \neq \{z\}$, for all n. Consider the sequence of mappings θ_n from ξ into $\mathcal{P}(\xi)$ given by $\theta_{n+1}(z) = \bigcup_{t \in \theta'_n(z)} B_n(t) = \mathcal{D}_{B_n}(\theta'_n(z))$ for $n > 0, z \in \xi$ and $\theta_0(z) = \{z\}$, for every $z \in \xi$. We define the integer N_X by $N_X = \max\{n : \mathcal{E}_{\theta_n}(X) \neq \emptyset\}$ for a given $X \in \mathcal{P}(\xi)$.

Definition 6. Consider $X \in \mathcal{P}(\xi)$. The spatially-variant (SV) morphological skeleton representation $R(X)$ of X is given by

$$R(X) = \{R_0(X), R_1(X), \cdots, R_{N_X}(X)\}, \tag{19}$$

where $R_n(X)$ is the spatially-variant morphological skeleton representation subset of order n given by

$$R_n(X) = \mathcal{E}_{\theta_n}(X) - \mathcal{D}_{B'_n}(\mathcal{E}_{\theta_{n+1}}(X)), \tag{20}$$

where $-$ denotes the set difference.

Theorem 6. The SV morphological skeleton representation is invertible. We have, for every $X \in \mathcal{P}(\xi)$,

$$X = R^{-1}(R(X)) = \bigcup_{n=0}^{N_X} \mathcal{D}_{\theta_n}(R_n(X)). \tag{21}$$

5.2.2. Algorithmic Analysis

Given a binary image X, the transformation $R(\bullet)$ results in the representation $R(X)$, which is a compressed version of image X. The representation $R(X)$ usually sustains additional processing determined by the desired application; e.g., coding and decoding for the transmission of $R(X)$ over a communication channel. In the remainder of this section, we assume that the channel is noiseless. Therefore, the receiver will be able to reconstruct the original image perfectly without error by using the inverse transformation $R^{-1}(\bullet)$.

Our goal is to construct the optimal structuring elements, which result in a minimum representation of the SV morphological skeleton. Given a binary image X, the trivial solution for the optimal structuring element would be the image itself. The translation-invariant and spatially-variant morphological skeleton representations would be identical and consist of 1 point. However, this is not a practical solution since it assumes that the image in known before its reconstruction from its morphological skeleton representation. We will therefore assume a known fixed library of structuring elements and construct the optimal spatially-variant structuring element mapping to minimize the cardinality of the morphological skeleton representation. Let X denote the original image and B a given structuring element. Table 2 describes an algorithm to construct the optimal structuring elements for the spatially-variant morphological skeleton representation. The algorithm is an iterative process. At each iteration, the algorithm selects the center of the dilated structuring element $NB = B \oplus \cdots \oplus B$ (N times) that maximally intersects the image, for some integer N. The union of these center points constitutes the SV morphological skeleton representation. The exact reconstruction of the original image is guaranteed given the set of center points and their corresponding integers N. The resulting spatially-variant morphological skeleton representation is compact, in the sense that the set $\{(z_i, N_i), i = 0, \cdots, k\}$ is not redundant; i.e., the reconstruction based on any partial subset of the resulting SV morphological skeleton representation would form a strict subset of the original image. The translation-invariant and spatially-variant morphological skeleton representations are shown in Figs. 3(b) and 3(c), respectively. The cardinality of the SV morphological skeleton representation is less than one third than that of its translation-invariant counterpart.

(a) (b) 162 points (c) 502 points

Figure 3. Morphological skeleton representation: (a) Original image; (b) SV morphological skeleton representation (162 points); (c) Translation-invariant morphological skeleton representation (502 points).

6. CONCLUSION

In this paper, we presented a general theory of spatially-variant mathematical morphology (SVMM) and showed its enormous potential through two important image processing applications: adaptive median filters for morphological restoration of noisy images and SV morphological skeleton representation. The proposed theory preserves the geometrical notion of the structuring function, which is inherent in translation-invariant morphology. We derived the spatially-variant umbra homomorphism theorem, which states that the umbra operation is a

Table 2. An algorithm to construct the optimal structuring elements for the spatially-variant morphological skeleton representation.

Given a binary image X, do the following:
1. Choose $N_0 = \max\{n : X \ominus nB \neq \emptyset\}$.
2. Let $X_e = X \ominus N_0 B$.
3. Choose $z_0 \in X_e$ such that $|\{z_0\} \oplus N_0 B|$ is maximal.
4. Let $X' = X - \{z_0\} \oplus N_0 B$.
5. Store the value of z_0 and N_0. Let $M_{N_0} = 0; k = 0$;
6. While $(X' \neq \emptyset)$ do the following:
   - $a.$ $M = 0; N = N_0; k = k + 1$;
   - $b.$ While$(|NB| > M$ & $N \geq 0)$
     - $-N = N - 1$
     - $-$ Let $X_e = X \ominus NB$
     - $-$ Choose $z_N \in X_e$ such that $|(\{z_N\} \oplus NB) \cap X'|$ is maximal
     - $-$ Let $M_N = |(\{z_N\} \oplus NB) \cap X'|$
     - $-$ $M = \max_{n=N_0 \cdots N} M_n$
     - $-$ Temporarily store z_N
   - $c.$ Store z_k and $N_k : |(\{z_k\} \oplus N_k B) \cap X'| = M$ and empty the temporarily stored z_N's.
   - $d.$ Let $X' = X' - \{z_k\} \oplus N_k B$

The SV morphological skeleton representation is then given by $R(X) = \bigcup_{i=0}^{k} \{z_i\}$.
The reconstructed image is $X = \bigcup_{i=0}^{k} \{z_i\} \oplus N_i B$.

homomorphism between SV binary morphology and SV gray-level morphology. In the first application, we investigated the relation between adaptive median filters and the basic SV morphological operators (i.e., SV erosion and dilation). Simulation results showed that the adaptive median filter removes the noise while preserving the important features of the original image. In the second application, we generalized the morphological skeleton representation to the SV morphological skeleton representation. We have also developed an algorithm for optimal selection of the spatially-variant structuring element mapping, which results in the minimum cardinality of the SV morphological skeleton representation. As a result of this investigation, we have complemented the elegant theory of spatially-variant mathematical morphology with powerful practical algorithms for image processing applications.

7. APPENDIX

Proof of Proposition 1. Let V be an umbra. Suppose $(x, y) \in \mathcal{E}_{\Theta^U}(V)$. Let $w \leq y$. We show that $(x, w) \in \mathcal{E}_{\Theta^U}(V)$. By definition of the SV binary erosion, we have

$$(x, y) \in \mathcal{E}_{\Theta^U}(V) \Longleftrightarrow \Theta^U(x, y) \subseteq V \Longleftrightarrow U[\Theta(x)] + w \subseteq U[\Theta(x)] + y \subseteq V \Longleftrightarrow (x, w) \in \mathcal{E}_{\Theta^U}(V).$$

A similar argument can be used to derive that $\mathcal{D}_{\Theta^U}(V)$ is an umbra.
Proof of the umbra homomorphism theorem a) It suffices to show that the umbra $\mathcal{E}_{\Theta^U}(U[f])$ is closed for every $f \in USC(\xi, \mathcal{T})$. Let $\{z_n = (x_n, y_n)\}_{n \in \mathbb{N}}$ be a sequence in $\mathcal{E}_{\Theta^U}(U[f])$ converging towards $z = (x, y)$. In other words, we have $x_n \to x$ (i.e., $\lim_{n \to \infty} x_n = x$) and $y_n \to y$. We need to show that $(x, y) \in \mathcal{E}_{\Theta^U}(U[f])$. We have

$$(x_n, y_n) \in \mathcal{E}_{\Theta^U}(U[f]) \quad \Longleftrightarrow \quad \Theta^U(x_n, y_n) \subseteq U[f], \ \forall n \Longleftrightarrow \ U[\Theta(x_n) + y_n] \subseteq U[f], \ \forall n.$$

Since Θ is sequentially continuous and $\Theta(x)$ is u.s.c., $\forall x \in \xi$, we have $\Theta(x_n) \to \Theta(x)$ in the sense specified by Serra in [Thorem XII-2, p. 429].[3] So, $\Theta(x_n) + y_n \to \Theta(x) + y$. Since the spaces $USC(\xi, \mathcal{T})$ and the space of umbras in $\xi \times \mathcal{T}$ are homeomorphic,[32] an u.s.c. sequence of functions $\{g_n\}$ converges towards g iff the sequence of its umbras $\{U[g_n]\}$ converges towards $U[g]$. Therefore, we have $U[\Theta(x_n)] + y_n \to U[\Theta(x)] + y$. Since

$U[\Theta(x_n)+y_n] \subseteq U[f]$, $\forall n$ and $U[f]$ is closed, we have from [Corollary 3][2] that $U[\Theta(x)+y] \subseteq U[f]$, which is equivalent to $(x,y) \in \mathcal{E}_\Theta(U[f])$.

b) Similarly, it suffices to show that the umbra $\mathcal{D}_{\Theta^U}(U[f])$ is closed for every $f \in USC(\xi, \mathcal{T})$. Let $\{z_n = (x_n, y_n)\}_{n\in\mathbb{N}}$ be a sequence in $\mathcal{D}_{\Theta^U}(U[f])$ converging towards $z = (x,y)$. We need to show that $(x,y) \in \mathcal{D}_{\Theta^U}(U[f])$. We have

$$\begin{aligned} & (x_n, y_n) \in \mathcal{D}_{\Theta^U}(U[f]) \Longleftrightarrow \Theta^{U'}(x_n, y_n) \cap U[f] \neq \emptyset \\ \Longleftrightarrow \quad & \exists (a_n, b_n) \in \Theta^{U'}(x_n, y_n) \cap U[f],\ \forall n \Longleftrightarrow (a_n, b_n) \in U[f] \text{ and } [\Theta'(x_n)](a_n) + b_n \geq y_n. \end{aligned} \tag{22}$$

Let $K_n = \mathrm{Spt}(\Theta'(x_n))$. By hypothesis, K_n is compact for all n. Moreover, since Θ' is sequentially continuous, K_n converges to $K = \mathrm{Spt}(\Theta'(x))$ in the sense specified in [Theorem 1-4-1, p. 13].[2] Therefore, there exists a compact set K_0 such that $K_0 \supseteq K_n$ for all n. Since $a_n \in K_n \subseteq K_0$, there exists a convergent subsequence $a_{n_k} \to a$. By Theorem [Theorem 1-2-2, p. 6],[2] we have $a \in K$. From the fact that Θ is sequentially convergent, we have $\Theta(a_{n_k}) \to \Theta(a)$. We have $x_{n_k} \to x$. So, from [Theorem XII-2],[3] we have

$$\limsup [\Theta(a_{n_k})](x_{n_k}) \leq [\Theta(a)](x). \tag{23}$$

Since f is u.s.c. we have

$$\limsup f(a_{n_k}) \leq f(a) \tag{24}$$

From Eq. (22), we have $y_n - [\Theta(a_n)](x_n) \leq b_n \leq f(a_n), \forall n$. In particular, $y_{n_k} - [\Theta(a_{n_k})](x_{n_k}) \leq b_{n_k} \leq f(a_{n_k})$. So

$$\limsup (y_{n_k} - [\Theta(a_{n_k})](x_{n_k})) \leq \limsup b_{n_k} \leq \limsup f(a_{n_k}) \tag{25}$$

since $\limsup$ of a sequence of real or integer numbers always exists. Let $b = \limsup b_{n_k}$. Combining Eqs. (23), (25) and (24), we have

$$y - [\Theta(a)](x) \leq b \leq f(a). \tag{26}$$

So $(a,b) \in U[f]$ and $[\Theta(a)](x) + b \geq y \Longleftrightarrow (x,y) \in \Theta^U(a,b) \Longleftrightarrow (a,b) \in \Theta^{U'}(x,y)$. Finally, $(a,b) \in U[f] \cap \Theta^{U'}(x,y) \Longleftrightarrow (x,y) \in \mathcal{D}_{\Theta^U}(U[f])$.

Proof of Proposition 2.

$$\begin{aligned} \mathcal{D}_\Theta(f) \leq g \quad & \Longleftrightarrow \quad \forall x \in \xi, \vee_{u\in\xi}\{f(u) + [\Theta(u)](x)\} \leq g(x) \Longleftrightarrow \forall x, u \in \xi, f(u) + [\Theta(u)](x) \leq g(x) \\ & \Longleftrightarrow \quad \forall x, u \in \xi, f(u) \leq g(x) - [\Theta(u)](x) \Longleftrightarrow \forall u \in \xi, f(u) \leq \wedge_{x\in\xi}\{g(x) - [\Theta(u)](x)\} \Longleftrightarrow f \leq \mathcal{E}_\Theta. \end{aligned}$$

Proof of Proposition 3. Consider $f \in USC(\xi, \mathcal{T})$. We have, for all $x \in \xi$,

$$[\mathcal{E}^*_\Theta(f)](x) \quad = \quad [-\mathcal{E}_\Theta(-f)](x) = - \wedge_{u\in\xi} \{-f(u) - [\Theta(x)](u)\} = \vee_{u\in\xi}\{f(u) + [\Theta(x)](u)\} = [\mathcal{D}_{\Theta'}(f)](x).$$

This is true for every $f \in USC(\xi)$. Hence, $\mathcal{E}^*_\Theta = \mathcal{D}_{\Theta'}$.

Proof of Proposition 4. the proof follows immediately from Definitions 1 and 2.

Proof of Proposition 5. The proof follows immediately from Definitions 4 and 5.

Proof of Proposition 6. Consider $f \in USC(\xi, \mathcal{T})$. From the definition of the SV gray-level opening and the umbra homomorphism theorem, we have

$$\Gamma_\Theta[\Gamma_\Theta(f)] \quad = \quad T[\mathcal{D}_{\Theta^U}[\mathcal{E}_{\Theta^U}(U[\Gamma_\Theta(f)])]] = T[\mathcal{D}_{\Theta^U}[\mathcal{E}_{\Theta^U}(\Gamma_{\Theta^U}(U[f]))]] = T[\Gamma_{\Theta^U}(\Gamma_{\Theta^U}(U[f]))] = T[\Gamma_{\Theta^U}(U[f])] = \Gamma_\Theta(f)$$

A similar argument can be used to prove the idempotence of the SV gray-level closing.

Proof of Theorem 2. Consider an increasing V-operator Ψ. Let $f \in USC(\xi, \mathcal{T})$. Let $f' = \vee_{\Theta\in\mathcal{K}(\Psi)} \mathcal{E}_\Theta(f)$. We show that $[\Psi(f)](x) \geq t \Longrightarrow f'(x) \geq t$, for some $t \in \mathcal{T}$. Consider the mapping Θ_f given by

$$\Theta_f(x) = \begin{cases} f - t, & \text{if } [\Psi(f)](x) \geq t; \\ \mathcal{I}, & \text{Otherwise.} \end{cases} \tag{27}$$

Then

$$\Psi(\Theta_f(x)) = \begin{cases} \psi(f) - t, & \text{if } [\Psi(f)](x) \geq t; \\ \mathcal{I}, & \text{Otherwise.} \end{cases} \tag{28}$$

$[\Psi(\Theta_f(x))](x) \geq 0$, for every $x \in \xi$. Thus $\Theta_f \in \mathcal{K}(\Psi)$. Assume that $[\Psi(f)](x) \geq t$, for some $x \in \xi$. Then $\Theta_f(x) = f - t$. So, $[\mathcal{E}_{\Theta_f}(f)](x) = \vee\{v : \Theta_f(x) + v \leq f\} \geq t$ since $t \in \{v : \Theta_f(x) + v \leq f\}$. Hence, $f^{'}(x) = \vee_{\Theta \in \mathcal{K}\ (\Psi)} \mathcal{E}_{\Theta}(f)(x) \geq t$.
Conversely, we show that $f^{'}(x) > t \Longrightarrow [\Psi(f)](x) \geq t$. We have

$$\begin{aligned} f^{'}(x) > t &\iff \bigvee_{\Theta \in \mathcal{K}\ (\Psi)} \mathcal{E}_{\Theta}(f)(x) > t \Longrightarrow \exists \Theta \in \mathcal{K}(\Psi) : \mathcal{E}_{\Theta}(f)(x) \geq t \iff \exists \Theta \in \mathcal{K}(\Psi) : \wedge_u \{f(u) - [\Theta(x)](u)\} \geq t \\ &\Longrightarrow \exists \Theta \in \mathcal{K}(\Psi) : f - \Theta(x) \geq t \Longrightarrow \exists \Theta \in \mathcal{K}(\Psi) : \Psi(f) \geq t + \Psi(\Theta(x)). \end{aligned}$$

Since $\Theta \in \mathcal{K}(\Psi)$, we have $\Psi[\Theta(x)](x) \geq 0$. So, $\Psi(f)(x) \geq t$.
Finally, we have showed that $\{x : [\Psi(f)](x) \geq t\} = \{x : f^{'}(x) \geq t\}$, for every $t \in \mathcal{T}$, i.e., $\Psi(f)$ and f' have the same cross-sections. This implies that $\Psi(f) = f^{'}$. This establishes the proof that a function-processing system is an increasing V-system iff it is the supremum of erosions by mappings in its kernel. The dual representation in terms of SV gray-level erosions follows easily by duality.
Proof of Proposition 7. Consider $X, Y \in \mathcal{P}(\xi)$ such that $X \subseteq Y$. Let $r = (n+1)/2$. Then $z \in med(X, B) \iff |X \cap B(z)| \geq r$. Since, $X \cap B(z) \subseteq Y \cap B(z)$, we have $r \leq |X \cap B(z)| \leq |Y \cap B(z)|$. Hence $z \in med(Y, B)$. So $med(X, B) \subseteq med(Y, B)$. Thus the spatially-variant binary median is an increasing operator.
The dual of the adaptive binary median filter is

$$med^*(X, B) \ = \ (med(X^c, B))^c = \{y : |X^c \cap B(y)| < (n+1)/2\} = \{y : |X \cap B(y)| \geq (n+1)/2\} = med(X, B).$$

Similar arguments can be used to derive the increasing and self-duality of the SV gray-level median filter.
Proof of Proposition 8. Let $med_B = med(\bullet, B)$. $Ker(med_B) = \{\theta : |\theta(z) \cap B(z)| \geq (n+1)/2$, for every $z \in \xi\}$. Let $\mathcal{A}$ be the $\binom{n}{\frac{n+1}{2}}$ subsets of B of cardinality $(n+1)/2$. We have $\mathcal{A} \subseteq Ker(\mathrm{med}_B)$. So, $\bigcup_{\theta \in \mathcal{A}} \mathcal{E}_\theta \subseteq \bigcup_{\theta \in Ker(\mathrm{med}_B)} \mathcal{E}_\theta$. On the other hand, for each $\theta \in Ker(\mathrm{med}_B)$, there exists $\theta_0 \in \mathcal{A}$ such that $\theta_0 \subseteq \theta$. So $\mathcal{E}_\theta \subseteq \mathcal{E}_{\theta_0}$. So, $\bigcup_{\theta \in Ker(\mathrm{med}_B)} \mathcal{E}_\theta \subseteq \bigcup_{\theta \in \mathcal{A}} \mathcal{E}_\theta$. Finally, we have $\bigcup_{\theta \in Ker(med_B)} \mathcal{E}_\theta = \bigcup_{\theta \in \mathcal{A}} \mathcal{E}_\theta$. The representation of the adaptive binary median filter as intersection of dilations by the transposed mappings in $\mathcal{A}$ follows by duality. Similar arguments can be used to derive the kernel representation of the SV gray-level adaptive median filter.
Proof of Theorem 6. From the definition of the SV skeleton representation, we have $\mathcal{E}_{\theta_n} = R_n \cup \mathcal{D}_{B_n'}(\mathcal{E}_{\theta_{n+1}})$ Let $\Upsilon_n = \Gamma_{\theta_n}(X)$. Applying $\mathcal{D}_{\theta_n}$ to the latter equation, we obtain

$$\begin{aligned} \Upsilon_n &= \mathcal{D}_{\theta_n}(R_n(X)) \cup \mathcal{D}_{\theta_n}\mathcal{D}_{B_n'}\mathcal{E}_{\theta_{n+1}} = \mathcal{D}_{\theta_n}(R_n(X)) \cup \mathcal{D}_{\mathcal{D}_{B_n}(\theta_n')}\mathcal{E}_{\theta_{n+1}} = \mathcal{D}_{\theta_n}(R_n(X)) \cup \mathcal{D}_{\theta_{n+1}}\mathcal{E}_{\theta_{n+1}} \\ &= \mathcal{D}_{\theta_n}(R_n(X)) \cup \Upsilon_{n+1}. \end{aligned} \tag{29}$$

Observe that $\Upsilon_{N_X+1} = \emptyset$. By iterating Eq. (29) for $n = 0, 1, \cdots, N_X$, we obtain $\Upsilon_0 = \bigcup_{n=0}^{N_X} \mathcal{D}_{\theta_n}(R_n(X))$. Observe that $\Upsilon_0 = \Gamma_{\theta_0}(X) = X$. Therefore, we obtain the theorem.

REFERENCES

1. J. Serra, *Image Analysis and Mathematical Morphology. Theoretical Advances*, vol. 2, Academic Press, New York, 1988.
2. G. Matheron, *Random Sets and Integral Geometry*, J.Wiley and Sons, New York, 1975.
3. J. Serra, *Image Analysis and Mathematical Morphology*, Academic Press, San Diego, Calif., 1982.
4. J. Goutsias and S. Batman, "Morphological methods for biomedical image analysis," in *Handbook of Medical Imaging, Progress in Medical Image Processing and Analysis*, M. Sonka and J. Fitzpatrick, eds., **3**, pp. 175–272, SPIE Optical Engineering Press, 2000.
5. P. Soille, "Mathematical morphology: a powerful technique for shape analysis," in *International Conference on Shape Modelling and Applications*, May 2001.
6. P. A. Maragos and R. W. Schafer, "Morphological skeleton representation and coding of binary images," *IEEE Trans. Acoust., Speech, Signal Processing* **34**, pp. 1228–1244, Oct. 1986.
7. G. Gordon, "Automated glass fragmentation analysis," in *Proc. of the SPIE, Machine Vision Applications in Industrial Inspection*, **2665**, (San Jose,CA), Feb. 1996.

8. A. Hanbury and J. Serra, "Analysis of oriented textures using mathematical morphology," in *OAGM*, **3**, pp. 49–52, (Graz, Austria), September 2002.
9. F. Safa and G. Flouzat, "Speckle removal on radar imagery based on mathematical morphology," *Signal Processing* **16**, pp. 319–333, 1989.
10. A. J. Cand, U. de Mendon Braga Neto, and E. C. de Barros Carvalho Filho, "A mathematical morphology approach to the star/galaxy characterization," *Journal of the Brazilian Computer Society* **3**, April 1997.
11. H. Heijmans and J. Goutsias, "Nonlinear multiresolution signal decomposition schemes. ii. morphological wavelets," *IEEE Transactions on Image Processing* **9**, pp. 1897 – 1913, Nov. 2000.
12. P. A. Maragos, "A representation theory for morphological image and signal processing," *IEEE Transactions on Pattern Analysis and Machine Intelligence* **II**(6), 1989.
13. T. Ikenaga and T. Ogura, "Real-time morphology processing using highly parallel 2-d cellular automata cam/sup 2/," *IEEE Transactions on Image Processing* **9**, pp. 2018–2026, Dec. 2000.
14. S. Beucher, J. Blosseville, and F. Lenoir, "Traffic spatial measurements using video image processing," in *Proc. SPIE. Intelligent Robots and Computer Vision*, **848**, pp. 648–655, Nov. 1987.
15. C. S. Chen, J. L. Wu, and Y. P. Hung, "Theoretical aspects of vertically invariant gray-level morphological operators and their application on adaptive signal and image filtering," *IEEE Transactions On Signal Processing* **47**, pp. 1049–1050, April 1999.
16. I. Masayasu, T. Masayoshi, and N. Akira, "Morphological operations by locally variable structuring elements and their applications to region extraction in ultrasound images," *Systems and Computers in Japan* **34**, 2003.
17. C. S. Chen, J. L. Wu, and Y. P. Hung, "Statistical analysis of space-varying morphological openings with flat structuring elements," *IEEE Transactions On Signal Processing* **44**, April 1996.
18. H. Heijmans and C. Ronse, "The algebraic basis of mathematical morphology - i: Dilations and erosions," *Computer Vision, Graphics and Image Processing: Image Understanding* **50**, pp. 245–295, 1990.
19. P. Maragos, "Affine morphology and affine signal models," in *Proc. of SPIE Image Algebra and Morphological Image Processing*, **1350**, pp. 31–43, (San Diego, CA), July 1990.
20. J. Roerdink, "Group morphology," *Pattern Recognition* , pp. 877–895, 2000.
21. H. Heijmans and C. Ronse, "The algebraic basis of mathematical morphology - ii: Openings and closings," *Computer Vision, Graphics and Image Processing: Image Understanding* **54**, pp. 74–97, 1992.
22. G. Birkhoff, *Lattice theory*, American Mathematical Society, Providence, Rhode Island, 1984.
23. G. Banon and J. Barrera, "Decomposition of mappings between complete lattices by mathematical morphology, part i. general lattices," *Signal Processing* **30**, pp. 299–327, Feb 1993.
24. M. Charif-Chefchaouni, *Morphological Representation of Non-Linear Operators: Theory and Applications.* PhD thesis, University of Illinois at Chicago, 1993.
25. M. Charif-Chefchaouni and D. Schonfeld, "Spatially-variant mathematical morphology," in *Proc. IEEE International Conference on Image Processing*, pp. 555–559, 1994.
26. C. Ronse, "Why mathematical morphology needs complete lattices," *Signal Processing* **21**, pp. 129–154, October 1990.
27. D. Stoyan, W. Kendall, and J. Mecke, *Stochastic Geometry and its Applications*, John Wiley & Sons, Berlin, Germany, 1987.
28. D. Schonfeld and J. Goutsias, "Optimal morphological pattern restoration from noisy binary images," *IEEE Transactions on Pattern Analysis and Machine Intelligence* **13**, pp. 14–29, 1991.
29. P. Maragos and R. Schafer, "Morphological skeleton representation and coding of binary images," *IEEE Transactions on Acoustics, Speech and Signal Processing* **34**, pp. 1228–1244, 1986.
30. D. Schonfeld and J. Goutsias, "Morphological representation of discrete and binary images," *IEEE Transactions on Signal Processing* **39**, pp. 1369–1379, 1991.
31. R. Kresch and D. Malah, "Morphological reduction of skeleton redundancy," *Signal Processing* **38**, pp. 143–151, September 1994.
32. P. Maragos, *A Unified theory of Translation-Invariant Systems with Applications to Morphological Analysis and Coding of Images.* PhD thesis, Georgia Institute of Technology, July 1985.